BRIEF COMMUNICATION



Airborne sub-pollen particles from rupturing giant ragweed pollen

Elizabeth A. Stone • Chamari B. A. Mampage • Dagen D. Hughes • Lillian M. Jones

Received: 17 October 2020/Accepted: 12 March 2021/Published online: 5 May 2021 © The Author(s) 2021

Abstract Ragweed pollen is a prevalent allergen in late summer and autumn, worsening seasonal allergic rhinitis and asthma symptoms. In the atmosphere, pollen can osmotically rupture to produce sub-pollen particles (SPP). Because of their smaller size, SPP can penetrate deeper into the respiratory tract than intact pollen grains and may trigger severe cases of asthma. Here we characterize airborne SPP forming from rupturing giant ragweed (*Ambrosia trifida*) pollen for the first time, using scanning electron microscopy and single-particle fluorescence spectroscopy. SPP ranged in diameter from 20 nm to 6.5 μm. Most SPP are capable of penetrating into the lower respiratory tract, with 82% of SPP < 1.0 μm, and

are potential cloud condensation nuclei, with 50% of SPP $< 0.20 \, \mu m$. To support predictions of the health and environmental effects of SPP, we have developed a quantitative method to estimate the number of SPP generated per pollen grain (n_f) based upon the principle of mass conservation. We estimate that one giant ragweed pollen grain generates 1400 SPP across the observed size range. The new measurements and method presented herein support more accurate predictions of SPP occurrence, concentration, and air quality impacts that can help to reduce the health burden of allergic airway diseases.

Supplementary Information The online version contains supplementary material available at https://doi.org/10.1007/s10453-021-09702-x.

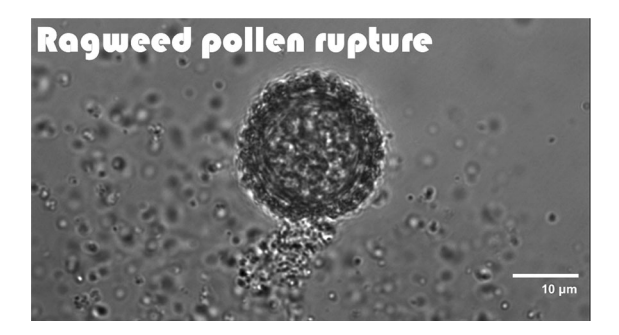
E. A. Stone (⋈) · C. B. A. Mampage · D. D. Hughes · L. M. Jones Department of Chemistry, University of Iowa, Iowa City, IA 52242, USA

e-mail: betsy-stone@uiowa.edu

E. A. Stone Department of Chemical and Biochemical Engineering, University of Iowa, Iowa City, IA 52242, USA



Graphic abstract Rupturing ragweed pollen releasing cellular components (right), viewed by an inverted light microscope.



Keywords Ambrosia · Sub-micronic · Pauci-micronic · Bioaerosol · Pollen fragment

1 Introduction

When exposed to high humidity or water, pollen grains can become engorged with water and osmotically rupture to release sub-pollen particles (SPP) to the atmosphere (Miguel et al., 2006; Schäppi et al., 1997; Taylor et al., 2002, 2004). SPP have been detected in atmospheric particles much smaller than the diameter of intact pollen, especially on days with rain by measurements of allergens (Habenicht et.al., 1984; Schappi et al., 1999) and chemical tracers (Hughes et al., 2020; Rathnayake et al., 2017). SPP have been observed to occur at the Earth's surface concurrent with precipitation and persist in the air for several hours after the rain ends, with peak concentrations occurring in convective thunderstorms (Hughes et al., 2020). Pollen rupturing is hypothesized to be enhanced by thunderstorms with strong winds, updrafts that carry pollen grains aloft to higher humidity where they rupture, and downdrafts that carry SPP to the surface (Taylor & Jonsson, 2004). SPP can deliver allergens deep into the respiratory tract and trigger severe asthma attacks (Schappi et al., 1999; Suphioglu et al., 1992). SPP are believed to be the major cause of "thunderstorm asthma" epidemics documented worldwide (D'Amato et al., 2019), including a catastrophic event in Melbourne, Australia, in 2016 in which a gust front storm in the midst of ryegrass pollen season triggered 9000 presentations at emergency rooms for severe and non-fatal asthma (Hew et al., 2019). SPP are also hygroscopic and can serve as cloud condensation nuclei (CCN) (Steiner et al., 2015), decreasing the frequency and intensity of precipitation (Wozniak et al., 2018).

We characterized the SPP released by giant ragweed, a prevalent and persistent allergen indigenous to North America that has spread to Europe and Asia. As ragweed's geographic range expands, so has its growing season (Oswalt & Marshall, 2008; Ziska et al., 2011) and atmospheric load in the USA (Ziska et al., 2019). While intact ragweed pollen grains are 15-20 µm in diameter, field studies have documented a paradox in which ragweed pollen antigens are observed in substantially smaller ambient aerosol particles (Busse et al., 1972; Solomon et al., 1983; Habenicht et al., 1984). For example, common ragweed (Ambrosia artemisiifolia) antigen (Amb a1) was observed in particles $< 5 \mu m$ in the Midwestern USA (Busse et al., 1972) and particles 2.5–10 µm in Poland (Grewling et al., 2016). Similarly, 27% ragweed DNA in particles < 10 μm in Germany was observed in particles < 2.5 μm (Muller-Germann et al., 2017). Our light microscopy reveals the ability of ragweed pollen to rupture to release cellular components upon exposure to water (TOC graphic).

Predicting the health and climate effects of atmospheric SPP requires accurate modeling of pollen rupture, particularly the number of SPP generated per pollen grain (n_f) and their size (Steiner 2020; Wozniak et al., 2018). Prior to this study, a single value for $n_{\rm f}$ was reported by Suphioglu et al. (1992) for a single rye grass pollen grain, which formed 700 SPP greater than 0.6 µm in diameter upon rupturing. This value provides an incomplete description of SPP, as field and laboratory studies demonstrate high concentrations of SPP with diameters $< 0.6 \mu m$ (Hughes et al., 2020; Taylor et al., 2002, 2004). Additionally, this single value does not account for variations in n_f across plant taxa, seasonal, or environmental conditions, which affects pollen grain shape, size, and composition. Herein, we characterize SPP released from giant ragweed (Ambrosia trifida) for the first time and develop and apply a new method to calculate n_f from measurements of SPP.



2 Materials and methods

SPP generated from fresh locally collected giant ragweed (Ambrosia trifida) pollen were characterized using our environmental chamber modeled after that of Taylor et al. (2002). Approximately five flowering stems of giant ragweed (20 cm) were attached to a steel rod and suspended inside a $25 \times 25 \times 30$ cm plexiglass chamber (Fig. S1). Intact pollen grains were dispersed by gently shaking the steel rod to simulate wind at 5-min intervals. SPP were generated by lightly misting the giant ragweed with 500 µL of deionized water delivered by a mechanically modified glass syringe concurrent with gentle shaking at 5 min intervals over 40 min. A small fan was placed inside the chamber to simulate light wind and a digital hygrometer (Taylor model 1732) monitored temperature (22 °C) and relative humidity, which was 61% during dry (intact pollen) and control experiments and increased to 89% following the water injections. Before each experiment, the chamber was purged with pressurized air passed through a HEPA filter (PALL Life Sciences) and hydrocarbon trap (Restek) air at 10 L min^{-1} for one hour.

Fluorescent particles with diameters 0.5-20 µm were characterized online by a single-particle fluorescence spectrometer (Wideband Integrated Bioaerosol Sensor, WIBS-NEO, Droplet Measurement Technologies) for the intact pollen, SPP, and background experiments (Hughes et al., 2020). Single-particle measurements were averaged to 10 second intervals. SPP were collected by a 13-stage Nano-MOUDI (125R NanoMoudi-IITM, MSP Corporation) onto polycarbonate filters (37 mm, 0.2 μm pore size, MilliporeSigma) or the Teflon after filter (47 mm, 0.2 µm pore size, MilliporeSigma). Samples were collected over 2 h 10 min with 24 water injections. Approximately 9×9 mm of polycarbonate filter was mounted onto aluminum SEM stubs using carbon tape (Ted Pella Inc.). The samples were sputter coated with gold (K550 Emitech Sputter Coater) and imaged with an accelerating voltage of 5 kV using a scanning electron microscope (Hitachi S-4800).

Intact giant ragweed pollen grains were collected on microscope slides coated with a thin layer of stopcock grease (Lubriseal), mounted with glycerin jelly containing a minimal amount of basic fuchsine, and sealed (Covergrip). Slides were viewed with a light microscope (Olympus BX-61) at the

20 × objective. Micrographs were analyzed in ImageJ (Schindelin et al., 2012) to determine the intact pollen grain diameter, circularity, and aspect ratio. Giant ragweed pollen grains, after exposure to water, were also viewed with an inverted microscope (Olympus IX-81) as shown in the graphical abstract.

3 Results and discussion

3.1 Characterization of giant ragweed SPP

Pollen rupturing was induced by misting flowering sprigs of giant ragweed with a fine spray of water at five-minute intervals, as indicated by the instantaneous appearance of fluorescent sub-micrometer SPP (Fig. 1a). The peak SPP number concentrations in the chamber (0.3–0.5 cm⁻³) were within the range of those observed in ambient air during convective thunderstorms $(0.3-1.3 \text{ cm}^{-3})$ by the same instrument (Hughes et al., 2020), indicating that environmentally relevant concentrations of SPP were produced in the chamber. The SPP fluoresced in one or more of the following excitation/emission channels leading to their designation as A-, B-, and/or C-type particles: (A) 280/310-400 nm, (B) 280/420-650 nm, and (C) 370/420-650 nm (Savage et al., 2017). SPP primarily consisted of ABC, AB-, BC-, and B-type particles that increased in number with decreasing particle size (Fig. 1b). Additionally, SPP fluoresced in fewer channels compared to intact pollen, which results from a combination of the loss of fluorophores during fragmentation and lower fluorescence intensities for smaller particles (Hernandez et al., 2016; Savage et al., 2017). In comparison with intact pollen grains (Fig. 1c), SPP decreased significantly in diameter (p < 0.001, Table S1). Peak SPP number concentrations occur at the lower limit of the WIBS instrument and imply high number concentrations of SPP $< 0.5 \mu m$.

SPP observed by SEM ranged in diameter from 20 nm to 6.5 μ m (Fig. 2). The mean diameter of 147 SPP was 560 nm and median diameter was 210 nm (Table S2). Of the observed SPP, 82% of the observed SPP were < 1.0 μ m, indicating that a large fraction of SPP are capable of penetrating the lower respiratory tract (Suphioglu et al., 1992). Additionally, 50% of observed particles were < 0.20 μ m, such that they are likely to act as cloud condensation nuclei (CCN) and



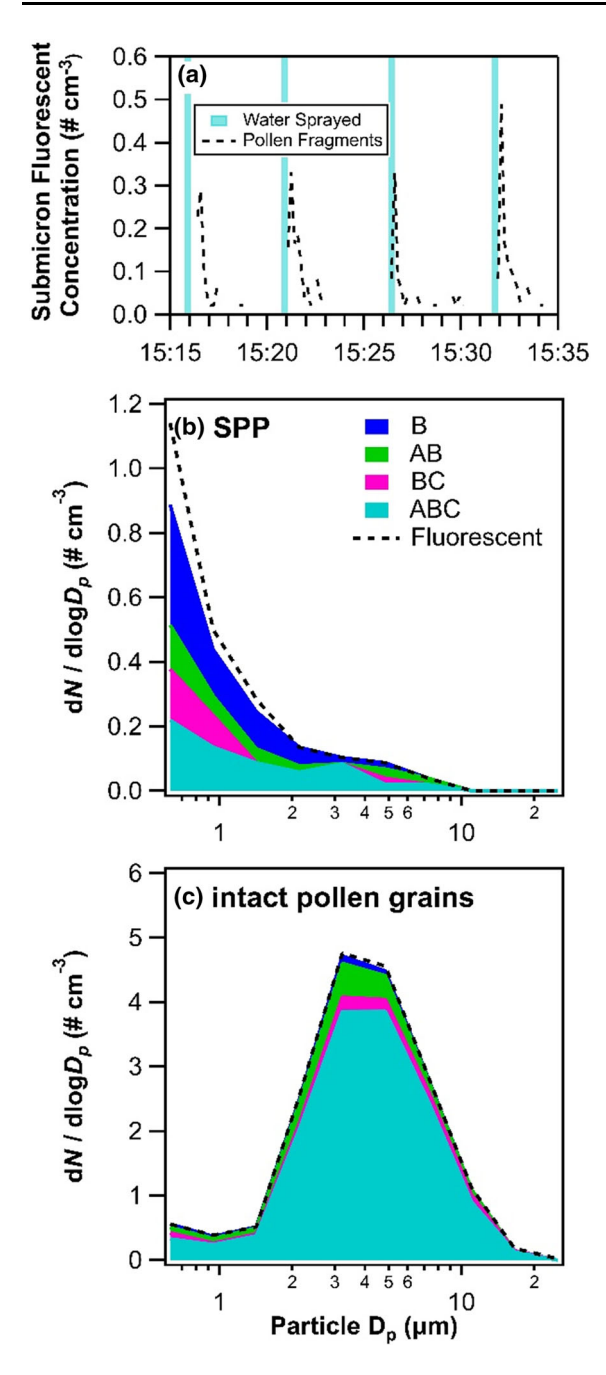


Fig. 1 a Sub-micrometer giant ragweed SPP observed by WIBS immediately after misting flowers with water at 5 min intervals. **b** The fluorescent particle size distribution and signatures are given for SPP and **c** intact pollen grains

impact cloud formation and precipitation (Steiner et al., 2015; Wozniak et al., 2018).

Giant ragweed SPP consisted of individual and agglomerated starch granules and other cellular

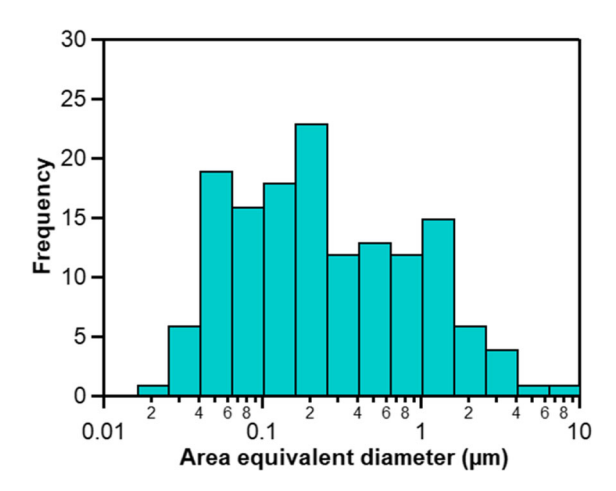


Fig. 2 Frequency distribution of SPP generated by rupturing giant ragweed pollen determined by SEM (n = 147)

components (Fig. 3), consistent with prior studies of SPP (Grote et al., 2000, 2001; Taylor et al., 2004). Morphology of the particles varied with particle diameter (Fig. S2). Below 0.5 μ m, SPP were rounder and more uniform, while above 0.5 μ m they were increasingly elongated and irregular in shape. The observation of pollen fragments from ragweed is significant in that ragweed is a major allergen that has a wide geographic impact and long growing season, making it a potentially large source of SPP to the atmosphere.

3.2 Method for determining the number of pollen fragments generated per pollen grain (n_f)

Total SPP number (N) were summed over the SPP particle size range, with the upper limit excluding intact pollen grains.

$$N = \sum_{i=1}^{k} n_i \tag{1}$$

SPP mass $(M; \mu g)$ was estimated as the product of volume (V_i) , and density (ρ_i) , with SPP volume estimated as spherical particles having the measured area equivalent diameter $(V_p = \pi D_p^3/6)$.

$$M = \sum_{i=1}^{k} V_{i} \rho_{i} \tag{2}$$

The mass per intact pollen grain (M_{grain} ; μg) was calculated from its volume using the diameter



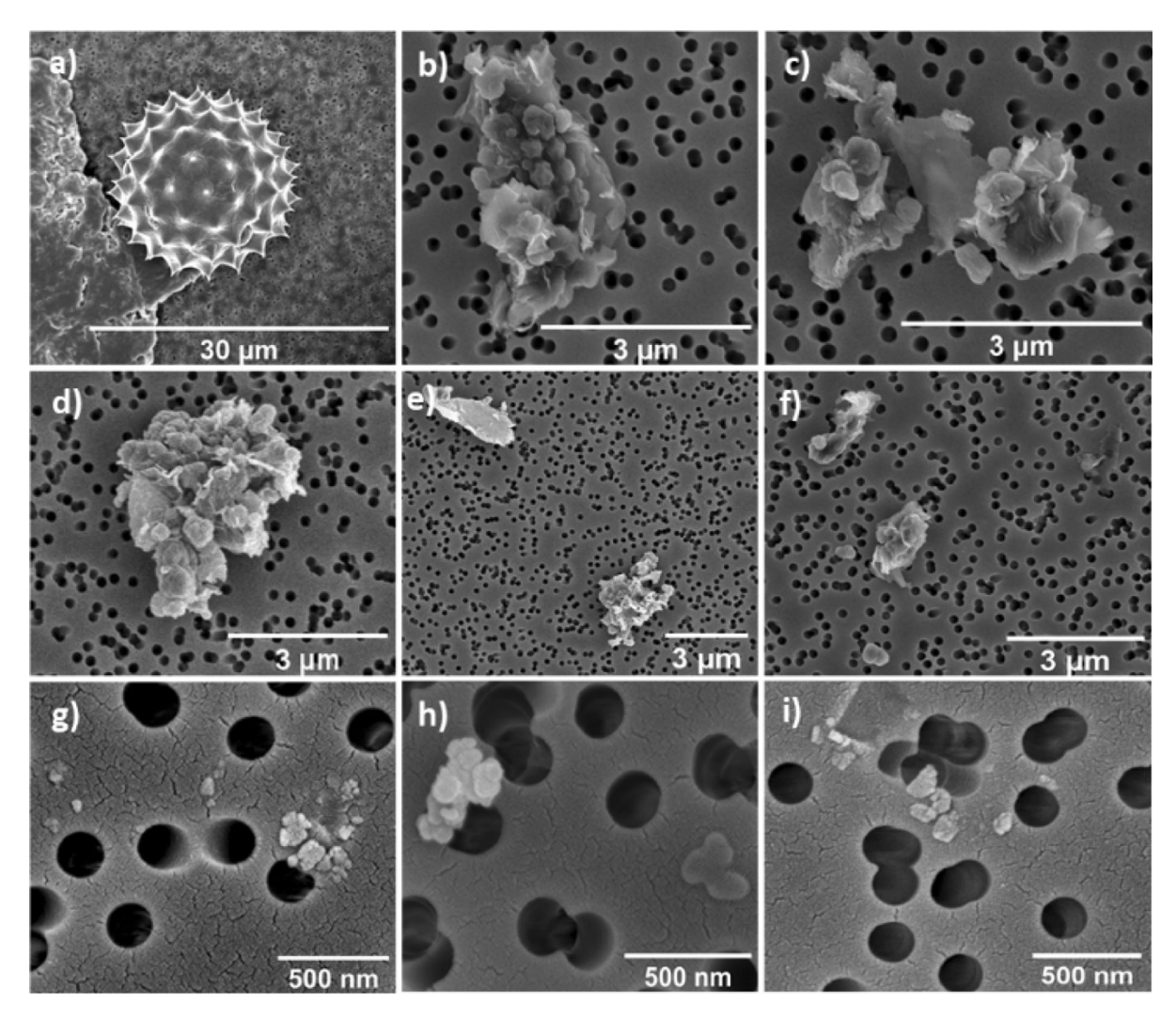


Fig. 3 a Scanning electron micrographs of giant ragweed pollen and b-i SPP. The polycarbonate substrates have a pore size of 0.2 μm

determined by light microscopy. Applying the principal of mass conservation, the number of grains that ruptured ($N_{\rm grains,rup}$) corresponds to

$$N_{\text{grains,rup}} = \frac{M}{M_{\text{grain}}} \tag{3}$$

The number of SPP generated per pollen grain is thus

$$n_{\rm f} = \frac{N}{N_{\rm grains,rup}} \tag{4}$$

In calculating $n_{\rm f}$, we assume conservation of pollen mass upon rupturing, no size-dependent particle losses, and that aggregate SPP density is equivalent to intact pollen grains. The latter assumption

conveniently cancels density terms from M and $M_{\rm grain}$ when calculating $n_{\rm f}$ by Eq. 4. It is reasonable to assume condensed-phase materials comprising pollen grains do not change appreciably in volume (i.e., are non-compressible). However, it is plausible that some SPP are enriched in starch granules that are denser (1.5 g cm⁻³) than intact ragweed pollen grains at 100% relative humidity (1.28 g cm⁻³) (Harrington & Metzger, 1963). This maximum error that this assumption may introduce (corresponding to the case in which SPP are exclusively starch granules) is 17% (the percent different in densities), but is expected to be much smaller, because large SPP that dominate M appear to be comprised of mixtures of pollen constituents (Fig. 3). Rather, the accuracy of $n_{\rm f}$



Plant taxa	Conditions	D _{grain} (μm)	D _{SPP} (μm)	n_f (size range)	References
Giant ragweed	Wetting	17.7	0.018–6.5	1400	This study
	wetting	17.7	0.6-6.5	400	This study
Bermuda grass	Wet/dry cycle	_	0.01–1	NA	Taylor et al. (2002)
Birch	Wet/dry cycle	18.6	0.01-0.7	NA	Taylor et al. (2004)
Chinese elm	Wet/dry cycle	29.8	1.5-8	530 ^a	Miguel et al. (2006)
Rvegrass	Wetting	30.1	0.6-2.5	700	Suphioglu et al. (1992)

Table 1 Summary of the number of SPP (n_f) generated per intact pollen grain by plant taxa, with the size range of SPP considered in the determination of n_f , conditions of pollen rupturing in the laboratory, diameter of the intact pollen grain, and references

determination depends heavily on that of N and M, which require consideration of the full size range of SPP, with SPP number highly influenced by particles $< 0.5 \, \mu m$ and SPP mass heavily weighted by particles $> 3 \, \mu m$. While this method is applied to single-particle SEM measurements, it is readily applied to other types of single particle measurements and airborne size distributions (see Supporting Information), making it broadly applicable to many measurement approaches.

3.3 Determination of n_f for giant ragweed

Our n_f method was applied to SEM measurements (Fig. 3), which accessed the broadest SPP diameter range and allowed ready distinction between SPP and intact pollen grains. In calculating M, we assume SPP are spherical and used the area equivalent diameter to help control for variation in size and shape. In calculating M_{grain} , we assumed a spheroidal shape, applied measured major diameter $17.7\,\pm\,0.9~\mu m$ (Fig. S3, Table S3) and mean aspect ratio of 1.04 \pm 0.03 (n = 21). Our resulting estimate of $n_{\rm f}$ indicates that one giant ragweed pollen grain ruptures into 1400 fragments ranging in diameter from $0.02-6.5 \mu m$ (Table 1). This n_f value is considered a lower limit, in case SPP < 200 nm are lost to substrate pores. Increasing the number of particles characterized will improve the accuracy of the estimated $n_{\rm f}$.

In making this estimate, we cover a much larger particle size range than has been examined before. The only prior measurement of $n_{\rm f}$ in ryegrass pollen measured no SPP < 0.6 μ m, and that a single ruptured ryegrass pollen released 700 starch granules ranging 0.6–2.5 μ m in diameter (Suphioglu et al.,

1992). Considering the same lower limit, we estimate that a giant ragweed pollen grain produces 380 SPP $> 0.6 \mu m$. The magnitude of this estimate gives us confidence in its reasonableness. The smaller $n_{\rm f}$ for giant ragweed likely results from its fivefold smaller volume compared to ryegrass pollen. Our method was also applied to Chinese elm pollen, using the SPP size distribution reported by Miguel et al. (2006), and returned an $n_{\rm f}$ value of 540. In doing so, we considered that Chinese elm pollen grains were spherical with a diameter of 29.8 µm and SPP above 1.5 µm due to the lower limit of their aerodynamic particle sizer. The minimum diameters measured by Miguel et al. (2006) and Suphioglu et al. (1992) likely underestimate $n_{\rm f}$ (Table 1) as they exclude the smaller SPP that are demonstrated to form from pollen rupturing by us (Figs. 1, 2) and others (Taylor et al., 2002, 2004). The developed method and new value of $n_{\rm f}$ for giant ragweed will advance atmospheric predictions of SPP from this plant taxa, but emphasize the need for accurate determination of n_f for other prevalent and allergenic pollen types across the entire size range of SPP.

Acknowledgements This research was supported by the National Science Foundation (AGS 1906091). We thank Thomas Peters for the loan of sampling equipment, Edward Dowling for assistance with SEM image processing, the University of Iowa Central Microscopy Research Facility (CMRF) for training and access to microscopes, and Chathurika Rathnayake for conducting inverted microscope experiments.

Open Access This article is licensed under a Creative Commons Attribution 4.0 International License, which permits use, sharing, adaptation, distribution and reproduction in any



^aDenotes values determined by retrospective data analysis using the method for n_f presented herein; NA marks experiments in which n_f could not be reliably determined because SPP > 1 μ m were not reported

medium or format, as long as you give appropriate credit to the original author(s) and the source, provide a link to the Creative Commons licence, and indicate if changes were made. The images or other third party material in this article are included in the article's Creative Commons licence, unless indicated otherwise in a credit line to the material. If material is not included in the article's Creative Commons licence and your intended use is not permitted by statutory regulation or exceeds the permitted use, you will need to obtain permission directly from the copyright holder. To view a copy of this licence, visit http://creativecommons.org/licenses/by/4.0/.

Author contributions EAS designed, directed, and supervised the research, developed the method for $n_{\rm f}$, analyzed data, and wrote the manuscript; CBAM conducted laboratory experiments, collected and analyzed SEM data, and wrote the manuscript; DDH conducted laboratory experiments, collected and analyzed WIBS data, and wrote the manuscript; LMJ collected and analyzed light microscopy images and wrote the manuscript.

References

- Busse, W. W., Reed, C. E., & Hoehne, J. H. (1972). Where is allergeic reaction in ragweed asthma 2 demonstration of ragweed antigen in airborne particles smaller than pollen. *The Journal of Allergy and Clinical Immunology*, 50(5), 289–293.
- D'Amato, G., Annesi-Maesano, I., Cecchi, L., & D'Amato, M. (2019). Latest news on relationship between thunderstorms and respiratory allergy, severe asthma, and deaths for asthma. *Allergy*, 74(1), 9–11.
- Grewling, L., Bogawski, P., Jenerowicz, D., Czarnecka-Operacz, M., Sikoparija, B., Skjoth, C. A., & Smith, M. (2016). Mesoscale atmospheric transport of ragweed pollen allergens from infected to uninfected areas. *International Journal of Biometeorology*, 60(10), 1493–1500.
- Grote, M., Vrtala, S., Niederberger, V., Valenta, R., & Reichelt, R. (2000). Expulsion of allergen-containing materials from hydrated rye grass (*Lolium perenne*) pollen revealed by using immunogold field emission scanning and transmission electron microscopy. *The Journal of Allergy and Clinical Immunology*, 105(6), 1140–1145.
- Grote, M., Vrtala, S., Niederberger, V., Wiermann, R., Valenta, R., & Reichelt, R. (2001). Release of allergen-bearing cytoplasm from hydrated pollen: A mechanism common to a variety of grass (Poaceae) species revealed by electron microscopy. The Journal of Allergy and Clinical Immunology, 108(1), 109–115.
- Habenicht, H. A., Burge, H. A., Muilenberg, M. L., & Solomon, W. R. (1984). Allergen carriage by atmospheric aerosol II ragweed-pollen determinants in submicronic atmospheric fractions. *The Journal of Allergy and Clinical Immunology*, 74(1), 64–67.
- Harrington, J. B., & Metzger, K. (1963). Ragweed pollen density. *American Journal of Botany*, 50(6P1), 532–539.

- Hernandez, M., Perring, A. E., McCabe, K., Kok, G., Granger, G., & Baumgardner, D. (2016). Chamber catalogues of optical and fluorescent signatures distinguish bioaerosol classes. Atmospheric Measurement Techniques, 9(7), 3283–3292.
- Hew, M., Lee, J., Susanto, N. H., Prasad, S., Bardin, P. G., Barnes, S., Ruane, L., Southcott, A. M., Gillman, A., Young, A., Rangamuwa, K., O'Hehir, R. E., McDonald, C., Sutherland, M., Conron, M., Matthews, S., Harun, N.-S., Lachapelle, P., Douglass, J. A., ... Thien, F. (2019). The 2016 Melbourne thunderstorm asthma epidemic: Risk factors for severe attacks requiring hospital admission. Allergy, 74(1), 122–130.
- Hughes, D. D., Mampage, C. B. A., Jones, L. M., Liu, Z., & Stone, E. A. (2020). Characterization of atmospheric pollen fragments during springtime thunderstorms. *Environ Sci Tech Let*, 7(6), 409–414.
- Miguel, A. G., Taylor, P. E., House, J., Glovsky, M. M., & Flagan, R. C. (2006). Meteorological influences on respirable fragment release from Chinese elm pollen. *Aerosol Science And Technology*, 40(9), 690–696.
- Muller-Germann, I., Pickersgill, D. A., Paulsen, H., Alberternst, B., Poschl, U., Frohlich-Nowoisky, J., & Despres, V. R. (2017). Allergenic Asteraceae in air particulate matter: Quantitative DNA analysis of mugwort and ragweed. *Aerobiologia*, 33(4), 493–506.
- Oswalt, M. L., & Marshall, G. D. (2008). Ragweed as an example of worldwide allergen expansion. *Allergy Asthma Clin Immunol*, 4(3), 130–135.
- Rathnayake, C. M., Metwali, N., Jayarathne, T., Kettler, J., Huang, Y., Thorne, P. S., O'Shaughnessy, P. T., & Stone, E. A. (2017). Influence of rain on the abundance of bioaerosols in fine and coarse particles. *Atmospheric Chemistry and Physics*, 17(3), 2459–2475.
- Savage, N. J., Krentz, C. E., Konemann, T., Han, T. T., Mainelis, G., Pohlker, C., & Huffman, J. A. (2017). Systematic characterization and fluorescence threshold strategies for the wideband integrated bioaerosol sensor (WIBS) using size-resolved biological and interfering particles. Atmospheric Measurement Techniques, 10(11), 4279–4302.
- Schäppi, G. F., Suphioglu, C., Taylor, P. E., & Knox, R. B. (1997). Concentrations of the major birch tree allergen Bet v 1 in pollen and respirable fine particles in the atmosphere. *The Journal of Allergy and Clinical Immunology*, 100(5), 656–661.
- Schappi, G. F., Taylor, P. E., Pain, M. C. F., Cameron, P. A., Dent, A. W., Staff, I. A., & Suphioglu, C. (1999). Concentrations of major grass group 5 allergens in pollen grains and atmospheric particles: Implications for hay fever and allergic asthma sufferers sensitized to grass pollen allergens. Clinical and Experimental Allergy, 29(5), 633–641.
- Schindelin, J., Arganda-Carreras, I., Frise, E., Kaynig, V., Longair, M., Pietzsch, T., Preibisch, S., Rueden, C., Saalfeld, S., Schmid, B., Tinevez, J.-Y., White, D. J., Hartenstein, V., Eliceiri, K., Tomancak, P., & Cardona, A. (2012). Fiji: An open-source platform for biological-image analysis. *Nature Methods*, 9(7), 676–682.
- Solomon, W. R., Burge, H. A., & Muilenberg, M. L. (1983).
 Allergen carriage by atmospheric aerosol I Ragweed pollen



- determinants in smaller micronic fractions. *The Journal of Allergy and Clinical Immunology*, 72(5 PART 1), 443–447.
- Steiner, A. L. (2020). Role of the terrestrial biosphere in atmospheric chemistry and climate. Accounts of Chemical Research, 53(7), 1260–1268.
- Steiner, A. L., Brooks, S. D., Deng, C. H., Thornton, D. C. O., Pendleton, M. W., & Bryant, V. (2015). Pollen as atmospheric cloud condensation nuclei. *Geophysical Research Letters*, 42(9), 3596–3602.
- Suphioglu, C., Singh, M. B., Taylor, P., Bellomo, R., Holmes, P., Puy, R., & Knox, R. B. (1992). Mechanism of grasspollen induced asthma. *Lancet*, 339(8793), 569–572.
- Taylor, P. E., Flagan, R. C., Valenta, R., & Glovsky, M. M. (2002). Release of allergens as respirable aerosols: A link between grass pollen and asthma. *The Journal of Allergy* and Clinical Immunology, 109(1), 51–56.
- Taylor, P. E., Flagan, R. C., Miguel, A. G., Valenta, R., & Glovsky, M. M. (2004). Birch pollen rupture and the release of aerosols of respirable allergens. *Clinical and Experimental Allergy*, 34(10), 1591–1596.
- Taylor, P. E., & Jonsson, H. (2004). Thunderstorm asthma. Current Allergy and Asthma Reports, 4(5), 409–413.

- Wozniak, M. C., Solmon, F., & Steiner, A. L. (2018). Pollen rupture and its impact on precipitation in clean continental conditions. *Geophysical Research Letters*, 45(14), 7156–7164.
- Ziska, L. H., Knowlton, K., Rogers, C., Dalan, D., Tierney, N., Elder, M. A., Filley, W., Shropshire, J., Ford, L. B., Hedberg, C., Fleetwood, P., Hovanky, K. T., Kavanaugh, T., Fulford, G., Vrtis, R. F., Patz, J. A., Portnoy, J., Coates, F., Bielory, L., & Frenz, D. (2011). Recent warming by latitude associated with increased length of ragweed pollen season in central North America. Proceedings of the National Academy of Sciences of the United States of America, 108(10), 4248–4251.
- Ziska, L. H., Makra, L., Harry, S. K., Bruffaerts, N., Hendrickx, M., Coates, F., Saarto, A., Thibaudon, M., Oliver, G., Damialis, A., Charalampopoulos, A., Vokou, D., Heidmarsson, S., Gudjohnsen, E., Bonini, M., Oh, J. W., Sullivan, K., Ford, L., Brooks, G. D., ... Crimmins, A. R. (2019). Temperature-related changes in airborne allergenic pollen abundance and seasonality across the northern hemisphere: A retrospective data analysis. *The Lancet Planetary Health*, 3(3), e124–e131.

